Artículo de Investigación. Revista Ciencia e Ingeniería. Vol. 47, No. 1 pp. 95-106, diciembre-marzo, 2026.
ISSN 1316-7081. ISSN Elect. 2244-8780 Universidad de los Andes (ULA)

Valorization of gamelote (megathyrsus maximus) as lignocellulosic biomass for a biorefinery

Valorización del gamelote (megathyrsus maximus) como biomasa lignocelulosica para una biorrefinería

Villanueva, Iván[1]*; Pereira, Juan Carlos[1]
[1]Laboratory of Petroleum, Hydrocarbons and Derivatives, University of Carabobo, Valencia, Venezuela**.**
**ivillanu@uc.edu.ve*

Abstract

The growing interest in generating and/or consuming products obtained with environmentally friendly technologies, using raw materials from renewable resources, is leading to a focus on residual and untapped biomass sources in the production of lignocellulosic materials. Megathyrsus maximus, an abundant and underutilized biomass widely distributed in our country, is the central focus of this research, which aims to establish its potential for large-scale lignocellulosic material production. To this end, the biomass was subjected to various physical and chemical stages, including cutting, drying, grinding, sieving, delipidation, delignification, and bleaching, to ultimately obtain cellulose. It was found that the drying process at 60°C for 4 hours is equivalent to one month of air drying under ambient conditions. After the refining process, 13.8% cellulose was obtained on a wet basis from the fed biomass. The cellulose obtained was characterized by infrared spectroscopy in comparison with commercial cellulose, demonstrating the quality of the treatment carried out. Furthermore, it was characterized by thermogravimetric analysis and polarized light optical microscopy, which revealed the crystalline nature of the cellulose fibers obtained. In the studied area, between 13.9 tons/ha and 26.9 tons/ha of fresh Megathyrsus maximus (MM) can be harvested, from which it is projected to obtain between 1.7 tons/ha and 3.3 tons/ha of cellulose from the planted MM, demonstrating the potential of Megathyrsus maximus for processing into lignocellulosic substrates.

Keywords: *Megathyrsus maximus, cellulose, lignocellulosic biomass, biorefinery.*

Resumen

El creciente interés en generar y/o consumir productos obtenidos con tecnologías respetuosas con el medio ambiente, utilizando materias primas procedentes de recursos renovables, está impulsando la concentración de biomasa residual y sin explotar en la producción de materiales lignocelulósicos. Megathyrsus maximus, una biomasa abundante y subutilizada, ampliamente distribuida en nuestro país, es el foco central de esta investigación, cuyo objetivo es establecer su potencial para la producción de materiales lignocelulósicos a gran escala. Para ello, la biomasa se sometió a diversas etapas físicas y químicas, incluyendo corte, secado, molienda, tamizado, deslipidización, deslignificación y blanqueo, para obtener finalmente celulosa. Se observó que el proceso de secado a 60 °C durante 4 horas equivale a un mes de secado al aire en condiciones ambientales. Tras el proceso de refinación, se obtuvo un 13,8 % de celulosa en base húmeda a partir de la biomasa alimentada. La celulosa obtenida se caracterizó mediante espectroscopia infrarroja en comparación con la celulosa comercial, lo que demuestra la calidad del tratamiento realizado. Además, se caracterizó mediante análisis termogravimétrico y microscopía óptica de luz polarizada, lo que reveló la naturaleza cristalina de las fibras de celulosa obtenidas. En el área de estudio, se pueden cosechar entre 13,9 y 26,9 toneladas/ha de Megathyrsus maximus (MM) fresco, de lo cual se proyecta obtener entre 1,7 y 3,3 toneladas/ha de celulosa a partir del MM plantado, lo que demuestra el potencial de Megathyrsus maximus para su procesamiento en sustratos lignocelulósicos.

Palabras clave*: Megathyrsus maximus, celulosa, biomasa lignocelulósica, biorrefinería.*

1 Introduction

Grasses are primarily composed of cellulose and hemicellulose, which constitute approximately 70% of the total biomass (dry basis), and lignin, which comprises between 10-30%(Heinze et al, 2018). This chemical composition varies according to the species, tissue type, growth stage, and growing conditions, and also includes lipids and other polysaccharides to a lesser extent (Ríos et al., 2021). The grass Megathyrsus maximus (MM), also known as Guinea grass, native to Africa, has spread to many other regions of the world (Bryan et al, 2003). It forms isolated clumps with thin, green leaves are shown in Figure 1. It is a fast-growing grass that can reach a height of up to 3 m. It can withstand strong winds and rain thanks to its thick, resistant stem (Álvarez et al, 2016).

It produces seed year-round, with peak production occurring during the dry season. Annually, gambeteen 2-6 tona/ha of dry biomass can be produced in relatively fertile soils, and this can be increased with optimized agricultural strategies (Aristega et al., 2021). MM has been used to prevent soil erosion and as a livestock feed crop, but it has already been replaced by other species. If not managed properly, it can become an invasive grass and have a negative impact on native plant communities, given its rapid ability to establish itself over other plants (Cabrera et al., 2015). In Venezuela, this species is widespread, with a national distribution of approximately 16%, being more concentrated in the state of Zulia and the central region of the country (Guevara et al., 2012).

Of the three main constituents of MM, cellulose represents the most abundant renewable polymeric resource available worldwide, and in the plant, it is located in the cell walls, primarily bound to hemicelluloses, lignin, and pectins (Figueiredo et al., 2010). Globally, most plant-based cellulose is derived from wood; however, in recent years, other non-timber plant species, industrial waste, and agricultural byproducts have been used. In this regard, cellulose has been obtained from paper mill sludge (He et al., 2009), cereal crop waste (Sun et al, 2004), Musaceae (Zuluaga et al, 2007), pineapple bagasse (Antonio et al., 2014), among others. It is also possible to obtain cellulose from algae such as Valonia (Baker et al., 1997) or through the extracellular activity of microorganisms such as Acetobacter, Agrobacterium, Rhizobia, or Sarcina (Jung et al., 2005). The type of source used influences the physical, morphological, and mechanical characteristics of the cellulose. It is worth noting that the composition of lignocellulosic substrates also varies depending on the source used (Gonzalez et al, 2022).

Cellulose, chemically, is a polysaccharide, a linear natural polymer whose monomers are primarily β-(1 → 4)-D-glucopyranose (glucose) structures. Each β-anhydroglucose (UAG) unit has three exposed hydroxyl groups, which are capable of forming inter- and intramolecular hydrogen bonds.[16] This allows the polymer units to assemble into a hierarchical system. First, they form fibrillar units approximately 1.5–3.5 nm in diameter, which then assemble into microfibrils (nanofibers) with diameters ranging from tens to hundreds of nanometers. Finally, somewhat more randomly, they form interconnected microfibrillar networks (microfibers) with diameters on the micrometer scale or larger. These structures contain alternating sequences of crystalline and amorphous zones and represent the basic units of the plant cell wall in familiar cellulosic materials such as wood and cotton (Perez, 2005; Klemm et al, 2005; Heinze et al, 2012; Morales, 2015).

Throughout this system, hydrogen bonds play a fundamental role, as they are primarily responsible for the intramolecular interactions between the hydroxyl groups of adjacent anhydroglucose units and the intermolecular interactions that form between one cellulose chain and an adjacent one (León-Fernández et al, 2014). This has a strong influence on its mechanical, physical, and chemical properties, such as solubility, OH group reactivity, and crystallinity, among others. Furthermore, there are axial interactions between the C-OH sheets and Van der Waals interactions that stack these sheets (Nishiyama et al., 2002; Nishiyama et al., 2003; Tashiro et al., 2005).

Although cellulose is a highly hydrophilic polymer, it is insoluble in water. The intensity of the aforementioned interaction forces confers high stability to the crystalline structure. Cellulose solubilization is achieved by promoting the appearance of amorphous regions, with the weakening of intermolecular hydrogen bonds and the achievement of a positive interaction of the solubilizing agent with the cellulose (Carreño et al., 2005).

2 Experimental procedure

Megathyrsus maximus was collected fresh from an area of approximately 1 hectare located near the Faculty of Experimental Sciences and Technology at University of Carabobo, with geographic coordinates latitude: 10.2797° N and longitude: -68.0069° W. Within this area, a 1 m² square was delimited, and all the Megathyrsus maximus clumps contained therein were collected. The ears of each clump were counted and cut approximately 10 cm from the root, which was not evaluated in this study.

2.1 Obtaining Cellulose from Megathyrsus maximus

The methodology for obtaining cellulose was based on previous studies (Canche, 2005; Moreno, 2007; Rodríguez et al., 2007; Castillo, 2008; Carrero, 2013; Minmunin et al., 2015) carried out using plant biomass (see Figure 1). The leaves were manually cut into small pieces and then dried, some at room temperature and others in an oven at 60°C, in order to comparatively evaluate mass loss. Grinding was carried out in a helical mill. The material was then pulverized in a blade processor and subsequently fractionated using sieves of different pore sizes [ASTM80 (0.177mm); ASTM60 (0.250mm); ASTM20 (0.833mm) and ASTM18 (1mm)].

Delipidation was carried out using solid-liquid extraction with hexane in a Soxhlet extractor and in a glass reactor under total reflux. Different particle sizes of the dried plant material and total reflux times of 2 and 4 h were evaluated in this process. The extracted fat content was determined using Equation 1.

$$\text{Extracted fat content} = \frac{\mathbf{mo-mf}}{\mathbf{mMM}} * 100 \qquad \text{(Eq. 01)}$$

mo: sample mass before extraction (g)
mf: sample mass after extraction (g)
mMM: net mass of Megathyrsus maximus sample (g)

The delignification stage was carried out using the alkaline peroxide method at 70°C, in two stages, where the lignins and hemicelluloses present in the biomass were removed. The dried biomass was subjected to a reaction with 25% w/v hydrogen peroxide and 12% w/v sodium hydroxide at a mass/volume ratio of 1:30 (biomass: volume of aqueous phase) with stirring at 250 rpm or higher. Subsequently, the sample was filtered through a cloth, the filtrate was reserved, and the lignocellulosic residue was washed and then bleached with alkaline peroxide. A 25% w/v H_2O_2 solution was added progressively to achieve a 30:1 liquor/biomass ratio. Finally, the resulting material was filtered and dried to quantify the cellulose obtained for use in subsequent stages. Each batch of black liquor was stored for later analysis.

The characterization of the obtained cellulose consisted of ash determination, thermogravimetric analysis, FT-IR spectroscopy, polarized light optical microscopy, and scanning electron microscopy. Commercial cellulose and all chemicals were analytical grade, purchased from Sigma-Aldrich.

2.2 Thermogravimetric Analysis (TGA)

Thermogravimetric analysis allows for the study of the thermal stability of the materials under study and was performed on a NETZSCH STA 409 PC thermobalance. These analyses were carried out under an argon atmosphere with a flow rate of 50 mL/min. A heating ramp of 10 °C/minute was used, from 30 °C to 450 °C.

2.3 Infrared Spectra Determination

The cellulose obtained was analyzed by Fourier Transform Infrared (FT-IR) spectroscopy and compared with the spectra obtained for cotton (the natural material with the highest cellulose content) and commercially available cellulose. For this purpose, the sample was placed on the dish designed for direct Fourier Transform Infrared Spectroscopy analysis in a Perkin Elmer Frontier FT-IR Spectrometer, in the spectral range between 400 and 4,000 cm^{-1}.

2.4 Analysis by Polarized Light Microscopy

A MOTIC BA310 POL trinocular Siedentopf-type microscope, inclined at 30° and rotatable 360°, was used. A 360° rotating analyzer was used to take polarized light images of the cellulose obtained from Megathyrsus maximus and of the commercially available cellulose. This was done to compare the morphology of both materials at the scales used.

2.5 Scanning Electron Microscopy Determination

The cellulose obtained was analyzed by Scanning Electron Microscopy using a JEOL JCM-6000 instrument. The voltage used was 15 kV, and the samples were placed in the holder covered with a thin film of gold.

3. Results and discussion

3.1 Collection of Megathyrsus maximus

In the collection of the tillers, 2073.2 g/m² and 2693.4 g/m² of fresh biomass of Megathyrsus maximus were obtained. The number of clumbs and the number of ears present in the samples taken are reported in Table 1, according to the methodology described.

Table 1. Collection of fresh Megathyrsus maximus in an area of 1 m^2

Clumb	Number of ears of corn	High ears of corn ± 0,2 (m)	Clumb Mass ± 0,1 (g)
1	6	1,7	231,5
2	14	1,7	525,4
3	10	2,2	360,7
4	11	2,0	435,1
5	9	1,8	310,6
6	21	2,0	830,2
Averages	**12**	**1,9**	**448,9**

As can be seen in Table 1, 6 clumb were obtained in the demarcated area, with a variable number of ears per clumb, as well as variable ear length. It is worth noting that the mass of *Megathyrsus maximus* per area is not uniform, but rather falls within a range of values. On average, the number of ears per tiller per m² was 12 ± 4, and their length was 1.9 ± 0.2 m.

To estimate the availability of MM per area, the smallest clump mass (as an unfavorable scenario) and the average mass of the clumps (as a favorable scenario) were considered. This indicates that between 13.9 tons/ha and 26.9 tons/ha of fresh MM can be harvested. If the mass obtained in the other sampled area (20.7 tons/ha) is included in the estimate, it can be observed that it falls within the proposed range. Other studies of fresh MM harvesting reported yields between 14 and 25 tons/ha, and some achieved up to 40 tons/ha (Aristega et al., 2021). Gomez et al. (2021) reported between 20.3 and 28.0 tons/ha of fresh MM after 40 and 60 days of growth, respectively (Gómez et al., 2021). The observed differences can be attributed to soil quality, climatic conditions, and the agricultural strategies employed when applying nutrients during planting (Cerdas, 2011). This result demonstrates the potential of the land adjacent to the laboratory where the research was conducted, where more than 6 hectares of Megathyrsus maximus (MM) are planted but not currently being utilized.

3.2 Drying of the Cut Megathyrsus maximus

The drying process was performed on the smallest clump. The root was removed, and the rest of the plant was cut into small pieces. This was divided into three (3) parts, and the final appearance can be seen in Figure 1. The mass

loss during the drying process under ambient conditions was determined.

Table 2 shows the mass variation of the MM during storage at ambient temperature over the study period.

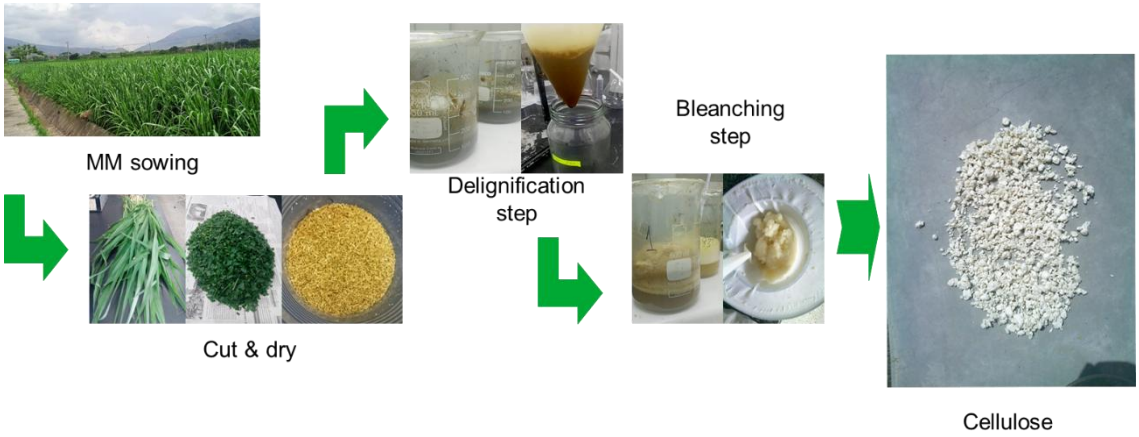

Figure 1. Production of cellulose from MM

It began with a total initial mass of 230.9 g, divided among the three samples. Additionally, the total mass loss of the evaluated clump was observed, reaching a net loss of 155 g in 180 days. On average, over a period of 6 months, the fresh MM sample had a percentage mass loss of 67 ± 1%. This percentage is mainly due to the water content in the plant material.

Table 2. Drying of fresh Megathyrsus maximus at room temperatura

Sample	Percentage mass loss per day (%)				
	0	**3**	**30**	**63**	**180**
1	0,0	31,2	68,1	71,5	68,9
2	0,0	28,3	64,5	68,1	65,3
3	0,0	35,8	66,3	69,8	67,2
Average	0,0	32± 3	66± 1	70± 1	67± 1

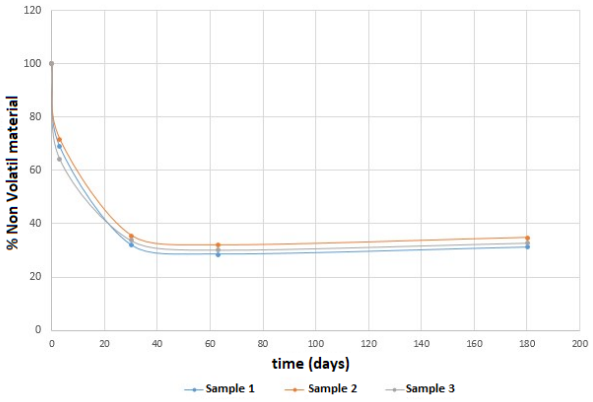

Figure 2. Variation of the non-volatile content of the plant material at ambient temperature

For comparison, the mass loss during the drying of Megathyrsus maximus ranged from 78.6% to 81.2%, measured after 40 and 60 days of drying, respectively (Gómez et al., 2021).

Similarly, the behavior of the non-volatile compounds present in the plant material is shown in Figure 2, as a function of the number of days exposed to ambient temperature.

It is worth noting that after 30 days, the change was minimal. At 6 months, a slight increase in mass was observed. Considering that plant material loses mass until it reaches equilibrium with its environment, this slight increase in mass at 6 months could be attributed to higher relative humidity at the time of weighing.

Furthermore, drying the fresh MM samples in an oven at 60 °C resulted in a mass loss of 65 ± 2%. That is, under the established conditions, the amount of mass obtained in 4 hours was equivalent to what would have taken approximately one (1) month at ambient temperature. This is very important when considering shortening the drying time, given the additional energy required for drying at a temperature higher than ambient. It is noteworthy that fresh MM has a high water content (Gonzalez et al., 2022; Dominguez, 2017) reported at 67.6% and 71.0%, respectively. This corresponds to the fact that water content can vary depending on the time of year and the climatic conditions present at the time of harvest. It is projected, then, that between 650 and 710 kg of water will evaporate for every ton of fresh MM processed, or, equivalently, between 9.1 and 17.6 tons of water per hectare of harvested land. Therefore, in large-scale processes, it would be an opportunity to consider studying the feasibility of condensing this water for use in subsequent processes.

Regarding the projected dry biomass of Megathyrsus maximus, it is projected to be between 4.8 and 9.3 tons/Ha. These levels are consistent with several studies that report ranges of 4.8 to 8.7 tons/Ha (Fortes et al., 2016); 2.0 to 3.9 ton/Ha (Milera et al., 2017); 5.8 to 8.7 ton/Ha (Pilco, 2017) and 1.3 to 6.2 ton/Ha (Homen et al., 2010), the latter in Venezuela (Edo. Miranda) in periods of 40 to 60 days of growth.

The values obtained are close to those reported for Megathyrsus maximus species in Colombia, where an average lipid content of 1.64% on a dry basis was obtained, and for species from Mexico with a lipid content of 1.6% on a dry basis.[41] A range of hexane extractables between 0.51 and 1.72% has also been reported (Milera et al., 2017).

Table 3. Sieving of the dried, ground, and crushed plant material

Sample	Percentage mass distribution of the sieved plant material (%m/m ±1)				
	Ø < 177 µm	**177 < Ø < 833 µm**	**833 < Ø < 1000 µm**	**1000 < Ø < 1400 µm**	**Ø > 1400 µm**
Dry MM	14	51	15	14	6

3.3 Grinding, crushing, and sieving of Megathyrsus maximus

The purpose of crushing the dried Megathyrsus maximus was to reduce the particle size to increase the exposed surface area, thus facilitating subsequent treatments. The mass distribution obtained after crushing and sieving, by particle size, is shown in Table 3. The most prevalent particle size range was between 177 and 833 µm.

In any case, the resulting mass distribution is associated with the time spent during crushing, the number of times it is repeated, the equipment used, and the energy applied. This distribution can be controlled by varying the time and frequency.

It is known that the energy required to reduce a plant source to a specific particle size is mainly influenced by the starting biomass (wood or grasses) (Cadoche, 1989) and the type of equipment used. Depending on the type of grinding employed and the type of material to be pretreated, the reduction in the final particle size desired is inversely proportional to the energy consumption required to achieve it, and its variation is not linear (Cadoche, 1989). As expected, the energy consumption to achieve a specific particle size is much higher when using wood as the starting source compared to when using grasses, such as Megathyrsus maximus. Similarly, greater energy or shear will be required to increase the proportion of particle sizes from larger to smaller.

3.4 Extraction of fatty components (delipidation)

It is known that fatty components are contained in the cells and cell walls of leaves, where they fulfill various roles in plants, such as hydrophobicity (waterproofing), energy storage, and signal transport, among others (Marcano, 2002). The lipid fraction obtained from grasses is mainly composed of galactolipids and phospholipids (86% molar) and, to a lesser extent, free fatty acids (3.1%), triglycerides (8.4%), and sterols (2.5%). The reported fatty acid composition was mostly unsaturated with 18 carbon atoms (75.3%) Carvajal-Tapia et al., 2023).

In this research, the removal of fat aimed to quantify the amount of its lipid content on a dry basis. Figure 3 shows the fat content extracted at different particle sizes from the plant material after 2 and 4 hours of extraction. It can be observed that the delipidation process with total reflux was favored when the particle size was smaller. The lipid content was extracted in the first two hours of reflux.

The highest fat content was obtained for a particle size of Φ < 177 µm, which can be attributed to the increased contact between the solvent and the solid due to greater disruption of the plant's epidermal tissue, resulting in greater solubility of the fats present in the plant matter Kumoro et al, 2021). In the Soxhlet extraction process, 1.90% was obtained in 4 h. After this stage, the solvent was recovered by vacuum distillation with a rotary evaporator, achieving a recovery percentage of 88%.

Figure 3. Fat content extracted from MM samples according to their size.

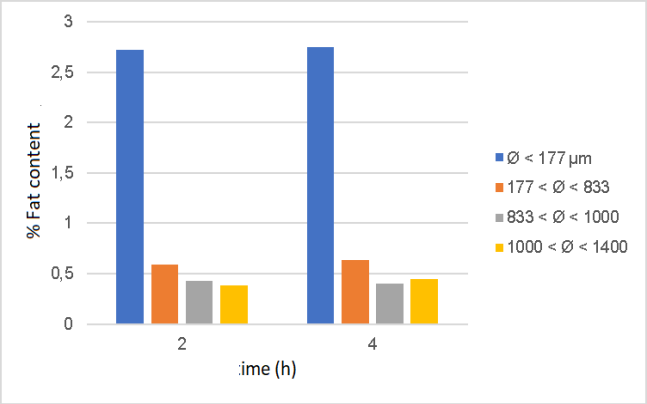

3.5 Delignification using the alkaline peroxide method

The final stage in obtaining cellulose consisted of removing hemicelluloses and lignins through the solid-liquid process already described, where the reaction raw material consisted of a dark brown liquor and a brown solid fraction that followed the bleaching process with H_2O_2. This liquid (black liquor) has an intense dark color, attributable to the activation of chromophoric groups present in the lignin. The reactions that occur are based on condensation and oxidation processes of phenolic groups, in which phenolates are obtained that promote its dissolution (Huang et al., 2019).

During the addition of H_2O_2, a large amount of foam was produced, promoted by the formation of oxygen from the reaction; therefore, the addition of H_2O_2 to the reaction medium had to be gradual to control the foam. During gravity filtration through a cloth filter, turbidity and sedimentation were observed in the filtered liquid fraction due to the passage of very fine cellulose particles. The filter cake was subjected to a second reaction with alkaline peroxide, decreasing the NaOH concentration to 6% and maintaining the H_2O_2 concentration at 25% w/w to improve the bleaching of the resulting cellulose.

After this stage, the mixture was filtered through a cloth. The filter cake (cellulose) was washed with distilled water until the wash water reached a neutral pH.

The percentage yield (dry basis) of cellulose, according to the particle size of the starting dry plant material, was higher for the largest particle size (43.00%) and 35.00% for the smallest size studied, values close to those reported (Gonzalez et al., 2022). This reduction in the efficiency of the cellulose production process is attributable to the particle size of the initial cellulose fibers, which turned out to be very fine particles that were not retained by the filtration mesh, as evidenced by sedimentation in the collection container of the reaction liquor. The cellulose obtained appears as agglomerated particles with a paper-like appearance as show in Figure 1. This agglomeration occurs during the filtration process.

It is worth noting that the biomass characterization of dry Megathyrsus maximus is summarized as follows: 13.2% moisture, 9.4% ash, 2.8% hexane extractables, 23% lignin, and 39.3% cellulose. Protein content was not determined; however, crude protein levels for Megathyrsus maximus have been reported in several countries, ranging from 13.95% to 16.53% in Colombia (Barragán-Hernández et al., 2019), 10.20% in Costa Rica (López-Herrera et al., 2019), 11.03% to 16.92% in Ecuador (Gomez et al., 2021), and from 19.76% to 16.43% in Venezuela (Homen et al., 2010), during a growth period of 21 to 35 days. Finally, based on the results obtained, the projected cellulose yield is between 1.7 and 3.3 tons/Ha planted with Megathyrsus maximus.

3.6 Thermogravimetric Analysis (TGA)

Thermogravimetric analysis allowed us to determine the stability of the cellulose samples as a function of temperature increase under an inert atmosphere. Figure 4 shows the thermogravimetric curves (TGA) and their corresponding derived thermogram (DTGA). These curves illustrate the variation of the percentage of residual mass with respect to the temperature increase up to 450°C.

It has been reported that the variation in the mass of lignocellulosic materials (cellulose, hemicellulose, and lignin) in a range of approximately 80 to 120°C is attributable to mass loss due to moisture (Reddy et al., 2018). This is observable in the DTGA curve in Figure 5, and Table 4 shows the mass loss values up to 120°C.

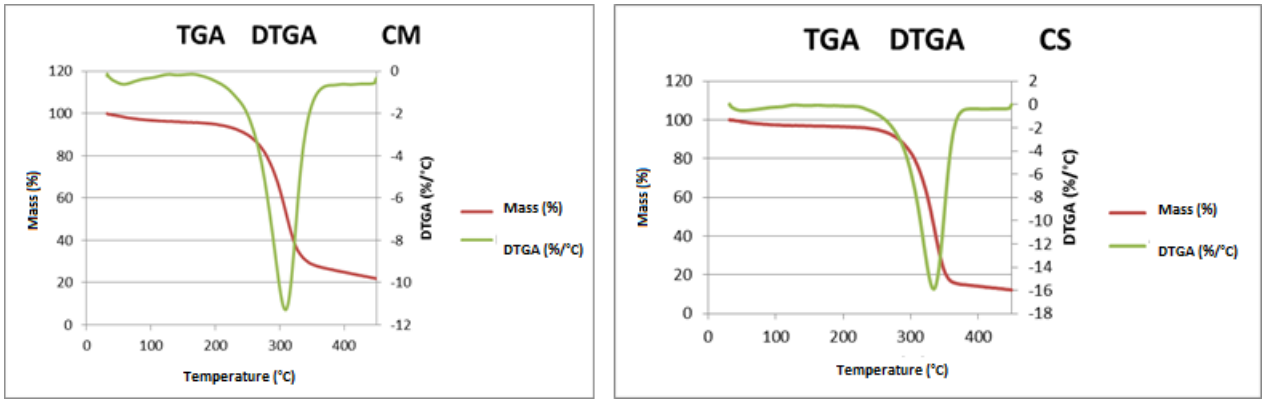

Figure 4. TGA and DTGA thermograms of cellulose from MM (left) and commercial cellulose (right)

Table 4. Thermogravimetric analysis of the celluloses

Cellulose	$T_{inicial}$ (°C)	T_{final} (°C)	T_{pico} (°C)	Percentage of mass lost to 120°C (%)	Percentage of mass lost to the T_{pico} (%)
MM	280	334	311	3,60	48,1
CS	305	355	336	2,85	57,5

Subsequently, the decomposition process of any hemicellulose present in the samples begins (above 190°C). This is followed by the decomposition of the cellulose, which overlaps with the decomposition of lignin (Yang et al., 2007).

The peak or average decomposition temperature (Tpeak) is represented by the inflection point in the thermogram and by the minimum reached in the DTGA curve. It should be noted that this material is composed of a distribution of molecules with different degrees of polymerization and under different crystalline arrangements; therefore, an average value will be obtained. These values are shown in Table 4.

Table 4 shows that at 120 °C, the percentage of mass loss was slightly higher for MM cellulose compared to commercial cellulose. In the former case, the mass loss was 3.60%, while for commercial cellulose it was 2.85%. This reduction is attributable to the elimination of moisture contained in the cellulose (Reddy et al., 2018). The mass loss at the average decomposition temperature was greater for commercial cellulose, at 57.5%, compared to MM cellulose, at 48.1%. Additionally, the initial decomposition temperature ($T_{initial}$) of MM cellulose began earlier than that of commercial cellulose. This greater decomposition was reached at a higher temperature in commercial cellulose compared to MM, indicating that commercial cellulose, comparatively, showed greater thermal stability. This may be associated with differences in the degrees of polymerization and crystallinity.

3.7 Characterization of Cellulose by FT-IR

Samples of the obtained cellulose and commercially available cellulose were analyzed by Fourier transform infrared spectroscopy (FTRI) and are showm in Figure 5.
In each of the spectra obtained, the characteristic absorption bands of the analyzed samples are observed. The absorption band at 3328 cm^{-1} is attributed to the stretching vibration of the inter- and intramolecular H-O hydrogen bonds, characteristic of those present in cellulose (Oh SY et al., 2005[a]; Moran, 2008; Fan et al., 2012). The band at 2896 cm^{-1} corresponds to the stretching of the sp^3-hybridized carbons corresponding to the methylene (CH_2) groups of cellulose (Fan et al., 2012). The absorption band at 1638 cm^{-1} indicates a certain amount of water adsorbed on the fiber, seen through the bending vibration of the OH group (Oh SY et al., 2005b). The band corresponding to the bending vibration of CH_2 (Oh SY et al., 2005b) is observed at 1423-1429 cm^{-1}. The band at 1315 cm^{-1} is attributed to the rocking vibration of the CH_2 group of carbon C_6 (Poletto, 2014). The band at 1159 cm^{-1} is attributed to the vibration of the β-glycosidic bond COC (Oh SY et al., 2005b).

The stretching vibrations of the C-O bond of ether groups appear in the range of 1050 to 1150 cm^{-1}, which are characteristic of the polymeric structure of cellulose (Coates, 2000). The intense band at 1026-1031 cm^{-1} is attributed to the stretching vibrations of the C-O bonds of primary alcohols Cichosz et al., 2022). At 896 cm^{-1}, the band is attributed to the stretching vibrations of the COC, CCO, and CCH bonds (Fan et al., 2012). Bands are observed at 1200 and 1500 cm^{-1} in the Megathyrsus maximus biomass, which disappear in the obtained cellulose and are also absent in commercial cellulose. These bands are attributable to the C-O stretching of aromatic alcohols characteristic of the lignin contained in the biomass (Coates, 2000).

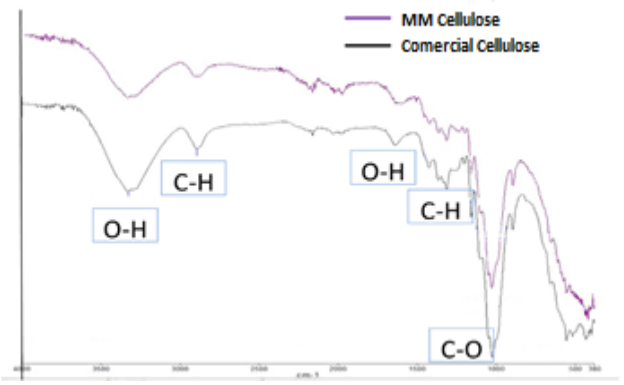

Figure 5. Comparison of functional groups present in cellulose obtained from Megathyrsus maximus with respect to commercial cellulose

Figure 5 shows a comparative analysis of the infrared spectra of MM cellulose, highlighting its similarity to the bands obtained from commercial cellulose, which was used for comparison. These results demonstrate the efficiency of the refining process used to obtain cellulose from MM biomass.

3.8 Polarized light optical microscopy

The commercial cellulose samples and the cellulose obtained from MM were analyzed by polarized light optical microscopy at magnifications of 40x and 100x (Figures 6 and 7). The commercial cellulose samples and the one obtained from MM were analyzed by polarized light optical microscopy, with a magnification of 40x and 100x (Figures 6 and 7).

It is worth noting that the observations made using this methodology reveal structures exhibiting birefringence, which is associated with the anisotropic crystalline structures present in cellulose. In the cellulose obtained from MM (Figure 6), aggregates of fibers of varying sizes are observed, structured longitudinally in parallel. The fibers of commercial cellulose have a uniform size distribution and shorter lengths than those obtained in the cellulose sample (Figure 7).

It is known that cellulose fibers form hierarchical structures, composed of cellulose chains distributed in crystalline and amorphous domains (Heinze, 2012). The crystalline structure confers high strength in mechanical properties, while the amorphous region contributes to elasticity. Furthermore, the amorphous region enhances the reactivity of cellulose.

3.9 Scanning Electron Microscopy

Figure 8 shows the microstructures formed by the cellulose fibers obtained from MM. They are arranged as loose filaments stacked on top of each other in three-dimensional space. They exhibit a linear conformation characteristic of cellulose microfibers, with variable thicknesses, mostly between 5 and 10 µm. Additionally, some show fibrillar aggregates with longitudinal channels on their surface. The cellulose is organized hierarchically, with each fiber composed of other, thinner fibers stabilized by hydrogen bond interactions present in the cellulose (Heinze, 2012).

The morphology observed in commercial cellulose shows fibers with greater thicknesses than those observed in cellulose from MM. The greater thickness and crystallinity observed in commercial cellulose fibers may confer greater thermal stability than those obtained from MM, which is consistent with the results obtained in the thermograms. This arrangement is composed of microfibrils stabilized by numerous hydrogen bonding forces.

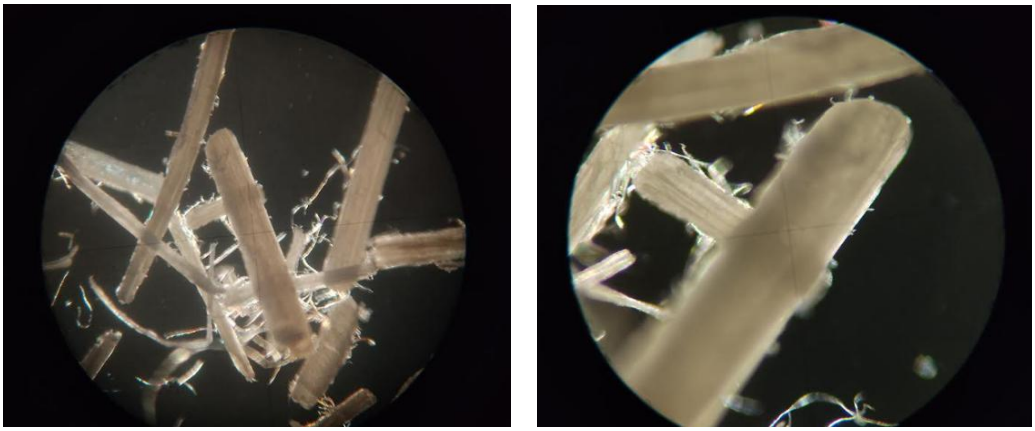

Figure 6. Polarized light microscopy image of cellulose obtained from Megathyrsus maximus. Left (40x), Right (100x)

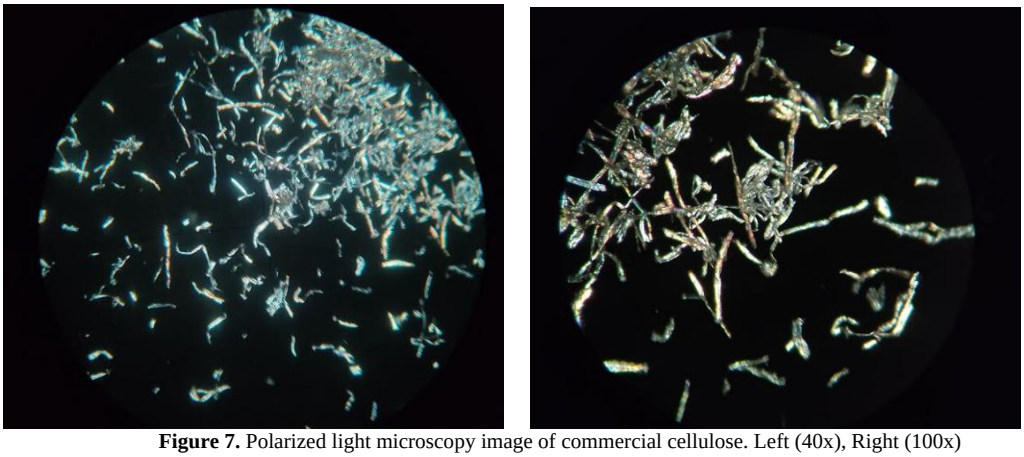

Figure 7. Polarized light microscopy image of commercial cellulose. Left (40x), Right (100x)

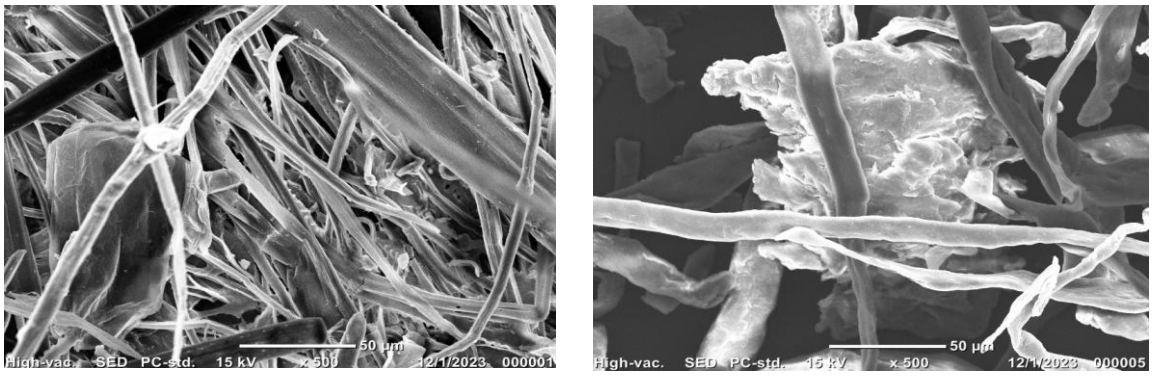

Figure 8. Scanning electron microscopy of Megathyrsus maximus cellulose from commercial cellulose (500x)

4 Conclusions

The production of cellulose from *Megathyrsus maximus* biomass was effective using physical processes such as cutting, drying, grinding, sieving, and solvent extraction of lipids, under chemical refining processes such as delipidization and delignification (bleaching) using 25% w/w H_2O_2 and 12% w/w NaOH.

Drying the pre-treated *Megathyrsus maximus* material at 60 °C for 4 h was equivalent to drying it in 30 days at room temperature.

The crystallinity and hierarchical structure of the cellulose fibers were evident by polarized light microscopy, and the refinement was demonstrated by visualizing disaggregated fibrillar structures using scanning electron microscopy, both in commercial cellulose and in that obtained from *Megathyrsus maximus.* FTIR spectroscopy confirmed the presence of the main characteristic bands in the cellulose obtained from *Megathyrsus maximus*, equivalent to those present in cotton cellulose and commercial cellulose.

The estimated availability of fresh *Megathyrsus maximus* per unit area (area adjacent to FACYT) is between 13.9 tons/ha and 26.9 tons/ha. The drying process (if the evaporated water is condensed) is estimated to yield between 9.1 and 16.5 tons/ha of water per unit area of planted land. Finally, the projected cellulose yield is between 1.7 and 3.3 tons/ha of planted *Megathyrsus maximus*.

References

Álvarez, G. R.; Vargas, J. C.; Franco, F. J.; Álvarez, P. E.; Samaniego, M. C.; Moreno, P. A.; Chacón, E.; García, A. R.; Arana, R. S. y Ramírez de la Ribera, J. L. (**2016**). Rendimiento y calidad del pasto Megathyrsus maximus fertilizado con residuos líquidos de cerdo.REDVET. Revista Electrónica de Veterinaria, Vol. 17 (6), pp. 1-9.

Antonio R., Ramos C., García R., Sandoval G. y Arellano L. (**2014**). Gel de carboximetilcelulosa (CMC) a partir del bagazo de piña. Ciencias de la Ingeniería y Tecnología, Handbook. ECORFAN., Valle de Santiago, Guanajuato. ISBN 978-607-8324-24-8.

Aristega, M. J. C., Murillo, R. A. L., Coronel, A. L. E., & Garaicoa, D. A. R. (**2021**). Producción y composición química de Megathyrsus máximus cultivares Tanzania y Mombasa bajo condiciones del subtrópico ecuatoriano. Ciencia Latina Revista Científica Multidisciplinar, Vol. 5 (4), pp. 6427-6443.

Baker, A., Helbert, W. Sugiyama, J. y M. Miles (**1997**). High-Resolution Atomic Force Microscopy of Native Valonia Cellulose I Microcrystals. J. Struct. Biol., Vol. 119, pp. 129-138.

Barragán-Hernández, W. A., y Cajas-Girón PhD, Y. S. (**2019**). Cambios bromatológicos y estructurales en Megathyrsus maximus bajo cuatro arreglos silvopastoriles. Ciencia y Tecnología Agropecuaria, Vol. 20 (2), pp. 231-258.

Bryan, K., y Surrey, W. (**2003**). Megathyrsus, a new generic name for panicum subgenus megathyrsus. Austrobaileya, Vol. 6, pp. 571–5743.

Cadoche L. y López G. D. (**1989**) Assessment of size reduction as a preliminary step in the production of ethanol from lignocellulosic wastes. Biological Wastes. Vol. 30, pp. 153-157.

Canche G., De los Santos J., y col. (**2005**). Obtención de Celulosa a Partir de los Desechos Agrícolas del Banano. TEG. Universidad Juárez Autónoma de Tabasco. México.

Carreño, S., y Murcia, L. (**2005**). Obtención de acetato de celulosa a partir de residuos celulósicos postconsumo. Universidad Industrial de Santander. Bucaramanga, Colombia, pp. 8-205.

Carrero, M. (**2013**). Factores que afectan la transformación de biomasa en bioetanol. Ingeniería y Sociedad UC. Vol. 8 (1), pp. 53-60.

Carvajal-Tapia J.I., Barahona-Rosales R., Castro-Montoya J., Arango J. y Vivas-Quila N.J. (**2023**). Nutritional and biomass evaluation of a Megathyrsus maximus collection in a dry tropical climate in Colombia Tropical Grasslands-Forrajes Tropicales, Vol. 11 (1), pp. 11–21.

Castillo, V. y Núñez, M. (**2008**). Evaluación de la factibilidad técnico-económica de una planta para producir celulosa a partir de la masa foliar del MM y del Jacinto de agua. TEG. Universidad de Carabobo. Venezuela.

Cerdas R. y Vallejos E. (**2011**). Disponibilidad de biomasa del pasto Guinea (Megathyrsus maximus) Tanzania con varias fuentes y dósis de nitrógeno en Guanacaste, Costa Rica. InterSedes: Revista de las Sedes Regionales, Vol. 12 (23), pp. 32-44. Consultado en https://revistas.ucr.ac.cr/index.php/intersedes/article/view/975

Cichosz S., Masek A. Dems-Rudnicka K. (**2022**) Original study on mathematical models for analysis of cellulose water content from absorbance/ wavenumber shifts in ATR FT-IR spectrum. Scientific Reports, Vol.12 (1), pp.19739.

Coates J. (**2000**). Interpretation of Infrared Spectra, A Practical Approach. In Encyclopedia of Analytical Chemistry R.A. Meyers (Ed.). pp. 10815–10837

Dominguez, A. (**2017**). Síntesis de una molécula con actividad interfacial partiendo de la celulosa extraída de la masa foliar del Megathyrsus maximus (MM). Estudio en diferentes medios de solventes. Obtenido de (Tesis pregrado) Universidad de Carabobo, Venezuela.

Fan, M., Dai, D., y Huang, B. (**2012**). Fourier transform infrared spectroscopy for natural fibres. Fourier transform: materials analysis, Vol. 3, pp. 45-68.

Figueiredo, J., Ismael, M., Anjo, C., & Duarte, A. (**2010**). Cellulose and derivatives from wood and fibers as renewable sources of raw materials. Topics in Current Chemistry, Vo. 294, pp. 117–128.

Fortes, D., Valenciaga, D., García, C. R., García, M., Cruz, A. M., & Romero, A. (**2016**). Evaluación de tres

variedades de Megathyrsus maximus en el período poco lluvioso. Cuban Journal of Agricultural Science, Vol. 50 (1), pp. 131-137.

Gómez V., J., Galarza, G., Pérez, J., y Moran, C. (**2021**). Rendimiento de biomasa del pasto Saboya (Megathyrsus maximus) con relación a dos frecuencias de corte. Magazine de las ciencias. Revista de investigación e innovación. Vol. 6 (2), pp. 55-63.

González, M., Pereira-Rojas, J., Villanueva, I., Agüero, B., Silva, I., Velasquez, I., Delgado B., Hernández J., Rodriguez G., Labrador H., Barros H., Pereira, J. (**2022**). Preparation and characterization of cellulose fibers from Megathyrsus maximus: Applications in its chemical derivatives. Carbohydrate Polymers, Vol. 296, pp. 119918.

Guevara E. y Espinoza F. (**2012**). Nuevos materiales forrajeros para la producción de leche y carne en las sabanas de Venezuela. Instituto Nacional de Investigaciones Agrícolas (INIA) Anzoátegui-Centro Nacional de Investigaciones Agropecuarias (CENIAP), Maracay. pp. 57-144. Consultado en: chrome-extension://efaidnbmnnnibpcajpcglclefindmkaj/http://www.avpa.ula.ve/eventos/ii_simposio_pastca2006/13.pdf

He, X., Wu, S., Fu, D., & Ni, J. (**2009**). Preparation of sodium carboxymethyl cellulose from paper sludge. Journal of Chemical Technology & Biotechnology: International Research in Process, Environmental & Clean Technology, Vol. 84 (3), pp. 427-434.

Heinze T. y Liebert T. (**2012**). Celluloses and Polyoses/Hemicelluloses. In: Polymer Science: A Comprehensive Reference. Matyjaszewski K and Möller M (eds.) Vol. 10, pp. 83–152. Amsterdam: Elsevier BV. ISBN 9780080878621

Heinze T., El Seoud O.A. y Koschella A. (**2018**). Production and Characteristics of Cellulose from Different Sources. In: Cellulose Derivatives. Springer Series on Polymer and Composite Materials. Springer, Cham. pp. 1-18.

Homen, M., Entrena, I., Arriojas, L., & Ramia, M. (**2010**). Biomasa y valor nutritivo del pasto Guinea Megathyrsus maximus (Jacq.) BK Simon & SWL Jacobs.ʿ Gamelote en diferentes períodos del año en la zona de bosque húmedo tropical, Barlovento, estado Miranda. Zootecnia Tropical, Vol. 28 (2), pp. 255-266.

Huang, J., Fu, S., y Gan, L. (**2019**). Lignin Chemistry and Applications. Amsterdam, Netherlands: Elsevier. ISBN 0128139633

Jung, J., Park, J. y H. Chang (**2005**). Bacterial cellulose production by Glyconacetobacter hansenii in an agitated culture without living non-cellulose producing cells. Enzyme Microb. Tech., Vol. 37, pp. 347-354.

Klemm D., Heublein B., Fink H-P. y Bohn A. (**2005**). Cellulose: fascinating biopolymer and sustainable raw material. Angew Chem Int Ed, Vol. 44 (22), pp.3358-3393.

Angelo, R., Meléndez, H., Villarroel, M., Rodríguez, P., Imbert, F. y Del Castillo, H., (**2017**). Study of the reaction of dry reforming of methane using mixed oxide perovskites type $La_xSr_{1-x}Ni_yAl_{1-y}O_3$. Revista Ciencia e Ingeniería, Vol. 38 (1), pp. 17-30.

Kumoro, A. C., Wardhani, D. H., Retnowati, D. S., Haryani, K., Yustika, S., & Fajar, T. A. (**2021**). Extraction of essential oil from ultrasound pre-treated citronella grass (cymbopogon Nardus) leaves by hydro-distillation method. Chemical Engineering Transactions, Vol. 87, pp. 643-648.

León-Fernández, V., Rieumont-Briones, J., Bordallo-López, E., López-Hernández, O. D., y García-Peña, C. M. (**2014**). Mecanismo de liberación de diclofenaco a partir de un copolímero entérico base celulosa. Revista CENIC Ciencias Químicas, Vol. 45 (1), pp. 096-0101.

López-Herrera, M., Rojas-Bourrillon, A., & Briceño-Arguedas, E. (**2019**). Sustitution of Megathyrsus maximus grass by square guineo and urea in silage mixtures. Agronomía Mesoamericana, Vol. 30 (1), pp. 179-194.

Marcano D. y Hasegawa M. (**2002**). Fitoquímica Orgánica. Consejo de Desarrollo Científico y Humanístico. 2da Ed. Venezuela.

Milera Rodríguez, M., Alonso Amaro, O., Machado Martínez, H. C., & Machado Castro, R. L. (**2017**). Megathyrsus maximus. Resultados científicos y potencialidades ante el cambio climático en el trópico. Avances en Investigación Agropecuaria, Vol. 21 (3), pp. 41.

Minmunin, J., Limpitipanich, P., y Promwungkwa, A. (**2015**). Delignification of elephant grass for production of cellulosic intermediate. Energy Procedia, Vol. 79, pp. 220-225.

Morales S. (**2015**). Hidrólisis ácida de celulosa y biomasa lignocelulósica asistida con líquidos iónicos. Tesis Doctoral. Universidad Autónoma de Madrid. España. Consultado en http://hdl.handle.net/10261/132717

Morán JI, Alvarez VA, Cyras VP, Vázquez A (**2008**) Extraction of cellulose and preparation of nanocellulose from sisal fibers. Cellulose Vol. 15, pp. 149–159.

Moreno, N. (**2007**). Obtención de acetato de celulosa a partir de la masa foliar del Jacinto de agua (Eichornia crassipes) proveniente del Lago de Valencia. TEG. Facultad de Ingeniería. Universidad de Carabobo. Venezuela.

Nishiyama Y., Langan P. y Chanzy H. (**2002**). Crystal Structure and Hydrogen-Bonding System in Cellulose Iβ from Synchrotron X-ray and Neutron Fiber Diffraction. J. Am. Chem. Soc., Vol. 124, pp. 9074–9082.

Nishiyama Y., Sugiyama J., Chanzy H. y Langan P. (**2003**). Crystal Structure and Hydrogen Bonding System in Cellulose Iα from Synchrotron X-ray and Neutron Fiber Diffraction. J. Am. Chem. Soc., Vol. 125, pp. 14300–14306.

Oh SY, Yoo D I., Shin Y, Kim H. C., Kim H. Y., Chung Y. S., Park W. H., Youk J. H. (**2005a**). Crystalline structure analysis of cellulose treated with sodium hydroxide and

carbon dioxide by means of X-ray diffraction and FTIR spectroscopy. Carbohydr Res, Vol. 340, pp. 2376–2391.

Oh SY, Yoo D I., Shin Y, Seo G (**2005b**) FTIR analysis of cellulose treated with sodium hydroxide and carbon dioxide. Carbohydr Res, Vol. 340, pp. 417–428.

Pérez, S. y Mazeau, K. (**2005**). Conformations, structures and morphologies of celluloses. In Polysaccharides: Structural Diversity and Functional Versatility; Dumitriu, S. Ed.; Marcel Dekker: New York, Vol. 1, pp. 41. ISBN 1420030825

Pilco Herrera, L. J. (**2017**). Comportamiento agronómico y composición química de variedades de Bruchiarias y Megathyrsus maximus" (Bachelor's thesis, Ecuador: La Maná: Universidad Técnica de Cotopaxi; Facultad de Ciencias Agropecuarias y Recursos Naturales; Carrera de Ingeniería Agronómica).

Poletto M, Ornaghi Júnior HL, Zattera AJ (2014) Native cellulose: Structure, characterization and thermal properties. Materials (Basel) Vol. 7, pp. 105–6119.

Reddy, K., Maheswari, C., Dhlamini, M., Mothudi, B., Kommula, V., Zhang, J., Zhang, J., y Rajulu, A. (**2018**). Extraction and characterization of cellulose single fibers from native african Napier grass. Carbohydrate Polymers, Vol. 188, pp. 85–91.

Ríos J. V., Santiago O. M. A., Barrera-Martínez I., Álvarez V. P., 1 Carrillo L. P., JoséAmadorHonorato S. J. A. (**2021**). Characterization of mombaza grass as raw material to produce bioethanol. Revista Mexicana Ciencias Agrícolas, Vol. 12, 2.

Rodríguez O. Luis M. (2007). Estudio del proceso de obtención de celulosa a partir del MM (panicum virgatum), a nivel de planta piloto, utilizando un extractor Soxhlet. TEG. FACYT. Universidad de Carabobo. Venezuela.

Sun, X., Sun, R., Su, Y. y J. Sun. y M. Wada (**2004**). Comparative study of crude and purified cellulose from wheat straw. J. Agric. Food Chem., 52: 839-847.

Tashiro, K. y Kobayashi, M. (**1991**). Theoretical evaluation of three-dimensional elastic constants of native and regenerated celluloses: role of hydrogen bonds. Polymer. Vol. 32, pp. 1516-1526.

Yang, H., Yan, R., Chen, H., Lee, D.H., y Zheng, C. (**2007**). Characteristics of hemicellulose, cellulose and lignin pyrolysis. Fuel, Vol. 86, pp. 1781-1788.

Yang, U. M. y Fujita, H. (**1997**). Changes in grass lipid fractions and fatty acid composition attributed to hay making. Japanese Journal of Grassland Science, Vol. 42 (4), pp. 289-293.

Zuluaga, R.; Putaux, J. L.; Restrepo, A.; Mondragon, I. y Gañán, P. (**2007**). Cellulose microfibrils from banana farming residues: isolation and characterization. Cellulose. Vol. 14 (6), pp. 585–592.

Received: *Aug 09th, 2025*

Accepted: *Nov 04th, 2025*

Villanueva Sequera, Iván José: *Bachelor's Degree in Chemistry, 2001, Full Professor, Chemistry Department at Faculty of Engineering, University of Carabobo, Carabobo, Venezuela.*

https://orcid.org/0000-0003-4527-2280

Pereira Antique, Juan Carlos: *PhD in Applied Sciences (ULA). Director at Laboratory of Petroleum, Hydrocarbons and Derivatives (PHD). Full Professor, Department of Chemistry at Faculty of Experimental Sciences and Technology, University of Carabobo, Carabobo, Venezuela. Industrial Consultant in Interfacial Phenomena.*

Email: jcpereir@uc.edu.ve

https://orcid.org./0000-0003-4600-726X